European Journal of Radiology 176 (2024) 111502

Contents lists available at ScienceDirect

European Journal of Radiology

journal homepage: www.elsevier.com/locate/ejrad

Research article

Radiating blood flow signal: A new ultrasound feature of thyroid carcinoma

Sha-Sha Huang [a,1], Zheng Yang [b,1], Bin Li [c], Zhi-Hao Jiang [a], Yang Tan [a], Duo-Duo Hao [d], Chun-Qiao Chen [e], Ying-Wei Wang [f], Jin-Yu Liang [a], Fu-Shun Pan [a], Yi-Hao Liu [c], Xiao-Yan Xie [a], Yi-Fan Zhu [g,*], Zhu Wang [a,*]

[a] Department of Medical Ultrasonics, Institute of Diagnostic and Interventional Ultrasound, the First Affiliated Hospital of Sun Yat-Sen University, Guangzhou, China
[b] Department of Pathology, The Seventh Affiliated Hospital of Sun Yat-Sen University, Shenzhen, Guangdong, China
[c] Clinical Trials Unit, The First Affiliated Hospital of Sun Yat-Sen University, Guangzhou, China
[d] Department of Medical Ultrasonics, Shenzhen Bao'an District Songgang People's Hospital, Shenzhen, Guangdong, China
[e] Department of Medical Ultrasonics, Bao'an Central Hospital, Shenzhen, Guangdong, China
[f] Department of Medical Ultrasonics, Guangzhou Concord Cancer Center, Guangzhou, China
[g] Department of Thyroid Surgery, The First Affiliated Hospital of Sun Yat-Sen University, Guangzhou, China

ARTICLE INFO

Keywords:
Ultrasound
Radiating blood flow
Thyroid carcinoma

ABSTRACT

Objective: To summary radiating blood flow signals and evaluate their diagnostic value in differentiating benign and malignant thyroid nodules.
Materials and methods: We retrospectively recruited consecutive patients undergoing US at 4 hospitals from 2018 to 2022. In a training dataset, the correlations of US features with malignant thyroid nodules were assessed by multivariate logistic analysis. Multivariate logistic regression models involving the ACR TI-RADS score, radiating blood flow signals and their combination were built and validated internally and externally. The AUC with 95% asymptotic normal confidence interval as well as sensitivity, specificity, negative predictive value (NPV), and positive predictive value (PPV) with 95% exact binomial confidence intervals were calculated.
Results: Among 2475 patients (1818 women, age: 42.47 ± 11.57; 657 men, age: 42.16 ± 11.69), there were 3187 nodules (2342 malignant nodules and 845 benign nodules). Radiating blood flow signals were an independent risk factor for diagnosing thyroid carcinoma. In the training set, the AUC of the model using the combination of radiating blood flow signals and the ACR TI-RADS score (0.95 95 % CI: [0.94, 0.97]; $P < 0.001$) was significantly higher than that of the ACR TI-RADS model (0.91 [0.89, 0.93]). In the two internal validation sets and the external validation set, the AUCs of the combination model were 0.97 [0.96, 0.98], 0.92 [0.88, 0.96], and 0.91 [0.86, 0.95], respectively, and were all significantly higher than that of the ACR TI-RADS score (0.92 [0.90, 0.95], 0.86 [0.81, 0.91], 0.84 [0.79, 0.89]; $P < 0.001$).
Conclusion: Radiating blood flow is a new US feature of thyroid carcinomas that can significantly improve the diagnostic performance vs. the ACR TI-RADS score.

1. Introduction

The diagnostic value of the color Doppler ultrasound (CDUS) in differentiating malignant and benign thyroid nodules has long been in dispute [1–3]. There was a preliminary report on the evaluation of thyroid nodules by CDUS as early as 1989, when increased vascularity, an important parameter of thyroid cancer was reported [4]. Then, Horvath et al [5] found that hypervascularization and penetrating vascularity were related to the high probability of malignancy, and the Thyroid Imaging Reporting and Data System (TIRADS) was built by

Abbreviations: AACE, American Association of Clinical Endocrinologists; ACR TI-RADS, American College of Radiology Thyroid Imaging Reporting and Data System; ATA, American Thyroid Association; AUC, area under the curve; BTA, British Thyroid Association; CDUS, color Doppler ultrasound; CEUS, contrast-enhanced ultrasound; ETA, European Thyroid Association; FNA, fine needle aspiration; HAIbrid, human artificial intelligence hybrid; KSThR, Korean Society of Thyroid Radiology; NPV, negative predictive value; PPV, positive predictive value; ROC, receiver operating characteristic; TBSRTC, the Bethesda System for Reporting Thyroid Cytopathology; US, ultrasound.

* Corresponding authors.
E-mail addresses: zhuyifan@mail.sysu.edu.cn (Y.-F. Zhu), wangzhu@mail.sysu.edu.cn (Z. Wang).
[1] SSH and ZY contributed equally as co-first authors.

https://doi.org/10.1016/j.ejrad.2024.111502
Received 7 November 2023; Received in revised form 25 March 2024; Accepted 12 May 2024
Available online 13 May 2024
0720-048X/© 2024 Elsevier B.V. All rights are reserved, including those for text and data mining, AI training, and similar technologies.

taking BI-RADS as a model in 2009. With the deepening of research, several TIRADSs based on gray-scale US, CDUS, contrast-enhanced US (CEUS) or their combination were developed for differentiating malignant and benign thyroid nodules [5–15], some of which suggested that CDUS features of thyroid nodules was important for diagnosing malignant thyroid nodules [5,8]. The 2009 American Thyroid Association (ATA) management guidelines indicated that increased intranodular vascularity of a thyroid nodule was associated with a higher likelihood of malignancy [6]. The 2014 British Thyroid Association (BTA) guidelines classify peripheral vascularity of nodules as a feature of benign nodules and intranodular vascularity as a feature of malignant nodules [8]. The 2016 American Association of Clinical Endocrinologists (AACE) guidelines also suggest that intranodular vascularization is a feature of intermediate-risk thyroid lesions [10]. However, some researchers have reported that CDUS does not accurately predict malignancy in thyroid nodules [2,3]. Moon et al [16] did not recommend the routine use of color Doppler and power Doppler US for thyroid nodules in the consensus statement. Furthermore, a meta-analysis of 14 prospective studies suggested that vascular flow rate and intranodular vascularity were not risk factors for thyroid malignancy in 2016 [17]. Subsequently, the 2016 Korean Society of Thyroid Radiology (KSThR) guidelines, the 2017 American College of Radiology (ACR) guidelines, the 2017 European Thyroid Association (ETA) guidelines, the 2020 Chinese Medical Association guidelines and the 2022 CEUS TI-RADS did not include the parameters of CDUS [11–15].

The CDUS features that were mainly focused on in previous studies were the vascular abundance and the distribution pattern of blood flow, such as increased vascularity, intranodular vascularization and peripheral vascularity. As research has progressed, different perspectives in terms of the diagnostic value of CDUS features have emerged. Recently, some studies about the morphological characteristics of blood flow in thyroid nodules assessed with CDUS have been reported. In 2022, a study using a human artificial intelligence hybrid (HAIbrid) integrating framework showed that blood flow signals that are vertically distributed around the nodule are closely associated with malignant thyroid nodules [18]. Moreover, a retrospective study showed that 36 thyroid nodules with spoke wheel blood flow signals were all papillary thyroid carcinomas, indicating that the spoke wheel blood flow signal is a highly specific sign of papillary thyroid carcinoma (with specificity as high as 100.0 %) [19]. It is a pity that the above studies on morphological characteristics of blood flow have not further assessed the diagnostic value of this feature for thyroid cancer.

Therefore, we conducted a retrospective study to comprehensively summary the morphological characteristics of blood flow in thyroid nodules, and we aimed to assess the diagnostic performance of radiating blood flow signals in identifying benign and malignant thyroid nodules.

2. Materials and methods

2.1. Participants

The study was a multicenter retrospective study approved by the Research Ethics Committee of the First Affiliated Hospital of Sun Yat-Sen University (2022-069). The requirement for informed consent was exempted, as the data were retrospectively collected.

Consecutive patients with thyroid nodules on US images examined by 5 radiologists were enrolled from January 2018 to October 2022 at four hospitals (the First Affiliated Hospital of Sun Yat-Sen University, Guangzhou, China; Songgang People's Hospital, Shenzhen, China; Concord Cancer Center, Guangzhou, China; Bao'an Central Hospital, Shenzhen, China). The inclusion criteria were as follows: (a) underwent US (grayscale US and CDUS) before surgery or fine needle aspiration (FNA); (b) a definitive pathological result indicating benignity or malignancy; and (c) an initial benign result of FNA and decreased or stable nodule size at US follow-up after 12 months or more. The exclusion criteria were as follows: (a) the presence of thyroid nodules that were previously treated by any local therapy; and (b) nodules without final pathological results, including those classified as Bethesda I, III, or IV according to the Bethesda System for Reporting Thyroid Cytopathology (TBSRTC).

2.2. US examination

The US examination was performed carefully by two radiologists (W. Z., 17 years of experience; P.F.S., 10 years of experience) at the First Affiliated Hospital of Sun Yat-Sen University and three radiologists (H. D.D., C.C.Q., and W.Y.W., all with at least 5 years of experience) at Songgang People's Hospital, Concord Cancer Center and Bao'an Central Hospital. According to the level of vascular abundance in thyroid nodules [6], the color scale bar was adjusted appropriately. The color scale bar was mainly set to a range of 3–8 cm/s in this study. The color Doppler gain was adjusted to maximize the signal and set just below the level of random background noise. Grayscale US images and CDUS images of multiple planes in the thyroid nodules were routinely obtained. All data were well kept and centralized. Grayscale US and CDUS were performed using the linear array transducers (10–14 MHz) of real-time US systems (Mindray DC-8, Shenzhen, China; Canon Aplio 1900, Tokyo, Japan; Philips Cx50, Amsterdam, the Netherlands; or GE Volusion E8, United States). The patient maintained a supine position with slight flexion of the neck. Grayscale US and CDUS images of thyroid nodules were acquired by carefully scanning both transversely and longitudinally. When thyroid nodules were detected, their composition, echogenicity, shape, margin, echogenic foci and morphological characteristics of blood flow were recorded. All images were exported in JPEG format.

2.3. Ultrasonography image analysis

In accordance with the ACR TI-RADS [12], we abstracted the following features from the grayscale US images: composition (cystic, spongiform, mixed cystic and solid, or solid), echogenicity (anechoic, hyperechoic, isoechoic, hypoechoic, or very hypoechoic), shape (wider-than-tall or taller-than-wide), margin (smooth, ill-defined, irregular, or lobulated, extrathyroidal extension), and echogenic foci (no calcification or large comet-tail artifacts, macrocalcification, rim calcification, or punctate echogenic foci). Additionally, we extracted the CDUS feature: radiating blood flow signals (present or absent). The radiating blood flow signals were defined as multiple color Doppler signals in the form of dots, strips or short rods that were distributed radially around or inside the nodules, which might have an area without blood flow inside the nodules (Fig. 1).

All images were independently reviewed by two experienced radiologists (P.F.S.; L.J.Y., 10 years of experience in thyroid US). In cases of disagreement, a consensus was obtained by re-evaluation by a third experienced radiologist (W.Z., 17 years of experience in thyroid US). The reliability of the final data was confirmed by a consistency analysis of the data reviewed independently by two experienced radiologists (Supplementary Table 1). To verify that the radiologists had a good understanding of the radiating blood flow signals after training (interpretation of morphological characteristics of blood flow in 20 static images and 20 dynamic videos of each form of radiating blood flow as well as operation training of CDUS in 20 thyroid nodules), 500 nodules were randomly selected before and after training for the consistency analysis of the radiating blood flow signals judged by each of 6 radiologists (A.J.G.L.Y.S., Y.Y.B., Z.M., F.J.Y., C.C.L., H.J.Y., all of whom were engaged in advanced studies from different hospitals and had at least 3 years of experience in thyroid US) with the experienced radiologist. All radiologists were blinded to the clinical history, radiological report, and pathological results.

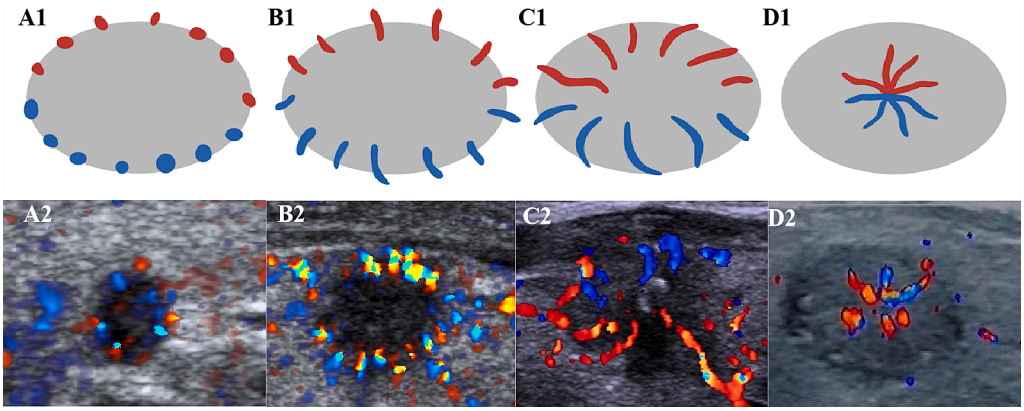

Fig. 1. Examples of typical radiating blood flow signals A 1–2) it is represented as multiple color Doppler signals in the form of dots distributed radially around the nodule, and a large area without blood flow can be seen inside the nodule; B 1–2) it is represented as multiple color Doppler signals in the form of strips or short rods distributed radially around the nodule, and the color Doppler signals can cross the boundary of the nodule; a large area without blood flow can be seen inside the nodule; C 1–2) it is represented as multiple color Doppler signals in the form of strips or short rods distributed radially inside the nodule, and the color Doppler signals can cross the boundary of the nodule; there may be an area of no blood flow in the center; D 1–2) it is represented as multiple color Doppler signals in the form of strips or short rods distributed radially inside the nodule and generally does not extend past the boundary of the nodule.

2.4. Statistical analysis

The chi-square test or Fisher's exact test was used to compare categorical variables, which are described as frequencies and percentages. The correlation of US features and malignant thyroid nodules was assessed by multivariable logistic regression. The diagnostic performances of the ACR TI-RADS score, the radiating blood flow signals and the combination of the ACR TI-RADS score and radiating blood flow signals in differentiating benign and malignant thyroid nodules were calculated and compared using the area under the curve (AUC) with 95 % asymptotic normal confidence interval as well as sensitivity, specificity, negative predictive value (NPV), and positive predictive value (PPV) with 95 % exact binomial confidence intervals. Additionally, receiver operating characteristic (ROC) curves were drawn. In the combination logistic model of the ACR TI-RADS score and radiating blood flow signals, radiating blood flow was scored as the coefficient of radiating blood flow signals divided by the coefficient of the ACR TI-RADS score and rounded to the nearest integer while keeping the ACR TI-RADS score unchanged [20]. Cohen's kappa correlation coefficients were calculated to assess the consistency of US features reviewed independently by two experienced radiologists. All statistical analyses were performed with Stata/MP software (version 14.0) and R-4.1.2 software. A two-sided $P < 0.05$ was considered to indicate a statistically significant difference.

3. Results

3.1. Patients

Finally, 3187 nodules from 2475 consecutive patients (1818 women, with a mean age of 42.47 ± 11.57 [SD], and 657 men, with a mean age of 42.16 ± 11.69) were included. Among all the nodules, 2443 nodules collected from January 2018 to December 2021 at the First Affiliated Hospital of Sun Yat-Sen University were randomly assigned to the training set or internal validation set 1 at a ratio of 7:3, and 425 nodules collected between January 2022 and October 2022 at the First Affiliated Hospital of Sun Yat-Sen University were included in internal validation set 2. For the external validation set, 239 patients with 319 nodules were

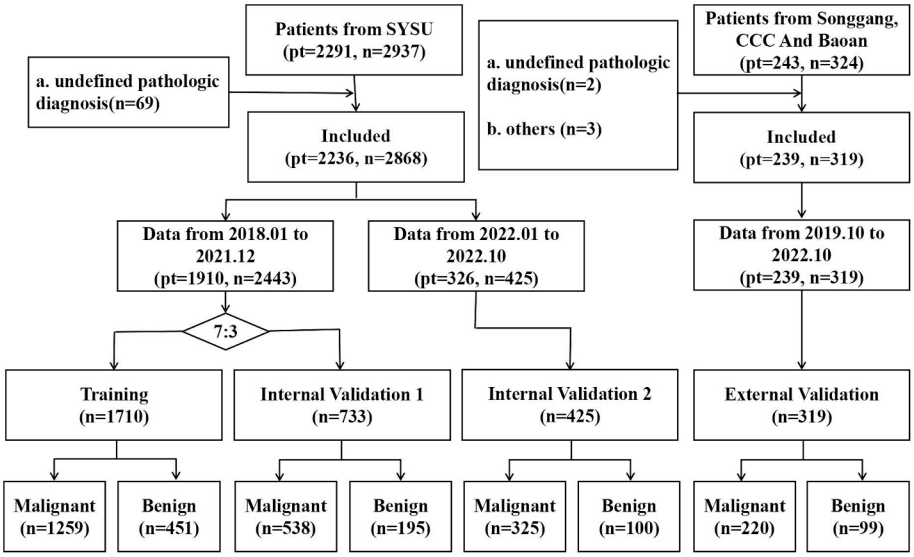

Fig. 2. Flow diagram of the included patients and number of thyroid nodules. SYSU = The First Affiliated Hospital of Sun Yat-Sen University, Songgang = Songgang People's Hospital (Shenzhen, China), CCC = Concord Cancer Center (Guangzhou, China), Baoan = Bao'an Central Hospital (Shenzhen, China), n = number of thyroid nodules, pt = number of patients.

collected from three other hospitals (Songgang People's Hospital, Shenzhen, China; Concord Cancer Center, Guangzhou, China; Bao'an Central Hospital, Shenzhen, China) (Fig. 2).

There were 2342 malignant nodules and 845 benign nodules. Malignant nodules with radiating blood flow accounted for 89.7 % and malignant nodules without radiating blood flow accounted for 10.3 %. Benign nodules with radiating blood flow accounted for 8.0 % and benign nodules without radiating blood flow accounted for 92 %.

In the malignant group, 98.8 % of nodules were papillary thyroid carcinomas, 0.6 % of nodules were follicular thyroid carcinomas, 0.4 % of nodules were medullary thyroid carcinomas, and 0.1 % of nodules were squamous cell carcinomas. In the benign group, the most prevalent benign nodule type was nodular goiters (87.7 %), followed by follicular thyroid adenoma (8.2 %); 2.8 % of nodules were nodular Hashimoto thyroiditis, 0.8 % of nodules were chronic granulomatous inflammation, and 0.5 % of nodules were subacute thyroiditis. The baseline characteristics are all shown in Tables 1-2 and Supplementary Tables 2-4.

3.2. Independent factors for diagnosing malignant thyroid nodules

In the training set, except for macrocalcification and rim calcification, significant differences were found between the two groups (all $P < 0.001$). Multivariable logistic regression analyses indicated that composition (OR: 4.12, 95 % CI [1.42, 11.95]; $P = 0.009$), echogenicity (hypoechoic, OR: 3.64, 95 % CI [2.06, 6.45]; $P < 0.001$; very hypoechoic, OR: 3.41, 95 % CI [1.54, 7.54]; $P = 0.002$), shape (OR: 2.48, 95 % CI [1.28, 4.82]; $P = 0.007$), margin (ill-defined, OR: 2.97, 95 % CI [1.44, 6.10]; $P = 0.003$; irregular or lobulated, OR: 2.32, 95 % CI [1.23, 4.40]; $P = 0.010$; extrathyroidal extension, OR: 8.41, 95 % CI [2.82, 25.13]; $P < 0.001$), punctate echogenic foci (OR: 4.69, 95 % CI [2.27, 9.72]; $P < 0.001$) and radiating blood flow signals (OR: 47.28, 95 % CI [28.22, 79.24]; $P < 0.001$) were independent predictors of thyroid carcinoma ($P < 0.01$ for all). Multivariable analyses of grayscale US and CDUS features for thyroid nodules are shown in Table 3.

3.3. Interobserver reliability of radiating blood flow signals

Consistency and accuracy analysis suggested that there was poor consistency and low accuracy among all six radiologists before training (Ka = 0.03–0.06, accuracy: 34.40 %-40.40 %) but good consistency and high accuracy (Ka = 0.58–0.91, accuracy: 86.40 %-96.40 %) after training. Numerical values are provided in Supplementary Table 5.

Table 1
Baseline data for the training set, internal validation set 1, internal validation set 2, and external validation set.

Parameter	Training set	Internal validation set 1	Internal validation set 2	External validation set	P value
No. of nodules	1710	733	425	319	
Sex					0.304
Female	1248 (73.0)	559 (76.3)	321 (75.5)	241 (75.5)	
Male	462 (27.0)	174 (23.7)	104 (24.5)	78 (24.5)	
Age (y)					0.966
Mean (SD)	43.2 (11.7)	42.9 (11.3)	42.9 (11.3)	43.4 (11.8)	
Median (IQR)	4.02 (34.0, 51.0)	42.0 (34.0, 52.0)	42.0 (34.0, 51.0)	42.0 (35.0, 50.0)	
Pathology					0.151
Malignant	1259 (73.6)	538 (73.4)	325 (76.5)	220 (69.0)	
Benign	451 (26.4)	195 (26.6)	100 (23.5)	99 (31.0)	

Note: Unless otherwise specified, presented data are the numbers of nodules, with percentages in parentheses.
SD = standard deviation; IQR = interquartile range; ACR TI-RADS = American College of Radiology Thyroid Imaging Reporting and Data System.

Table 2
Pathologic diagnosis and morphological characteristics of blood flow in 3187 thyroid nodules.

	Radiating blood flow signals		Total
	Present	Absent	
Malignant nodules	2101 (89.7)	241 (10.3)	2342
Papillary thyroid carcinoma	2083 (90.1)	230 (9.9)	2313
Follicular thyroid carcinoma	7 (53.8)	6 (46.2)	13
Medullary thyroid carcinoma	7 (70.0)	3 (30.0)	10
Squamous cell carcinoma	3 (100.0)	0 (0)	3
Lymphoma	0 (0)	2 (100.0)	2
Small cell neuroendocrine carcinoma	1 (100.0)	0 (0)	1
Benign nodules	68 (8.0)	777 (92.0)	845
Nodular goiter	50 (6.7)	691 (93.3)	741
Follicular thyroid adenoma	6 (8.7)	63 (91.3)	69
Nodular Hashimoto thyroiditis	6 (25)	18 (75)	24
Chronic granulomatous inflammation	5 (71.4)	2 (28.6)	7
Subacute thyroiditis	1 (25.0)	3 (70.0)	4

Note: Unless otherwise specified, presented data are the numbers of nodules, with percentages in parentheses.

3.4. Diagnostic Performance of the Combination of Radiating Blood Flow Signals and the ACR TI-RADS Score

In this study, the regression coefficients of the ACR TI-RADS score and radiating blood flow signals were 0.52 (95 % CI: 0.43, 0.60; $P < 0.001$) and 3.46 (95 % CI: 3.02, 3.90; $P < 0.001$), respectively. Since the ACR TI-RADS score remained the same, the radiating blood flow signals were assigned 7 points (Supplementary Table 6).

In the training set, there were no differences in the AUC of the radiating blood flow signals (0.91 [95 % CI: 0.89, 0.92]) and the ACR TI-RADS score (0.91 [95 % CI: 0.89, 0.93]; $P = 0.923$). The AUC of the combination of radiating blood flow signals and the ACR TI-RADS score was 0.95 [95 % CI: 0.94, 0.97], which was significantly larger than that of the ACR TI-RADS score alone ($P < 0.001$) (Fig. 3).

In internal validation set 1, no statistically significant difference was found between models using radiating blood flow signals (0.92 [95 % CI: 0.90, 0.94]) and the ACR TI-RADS score (0.92 [95 % CI: 0.90, 0.95]; $P = 0.859$). The AUC of the combination model using radiating blood flow signals and the ACR TI-RADS score (0.97 [95 % CI: 0.96, 0.98]) was significantly larger than that of the model using the ACR TI-RADS score alone ($P < 0.001$) (Fig. 3).

In internal validation set 2, compared with the model using the ACR TI-RADS score (0.86 [95 % CI: 0.81, 0.91]), the AUC of the model using radiating blood flow signals (0.90 [95 % CI: 0.86, 0.94]; $P = 0.072$) was nominally higher, but the difference was not statistically significant. The AUC of the model using the combination of radiating blood flow signals and the ACR TI-RADS score (0.92 [95 % CI 0.88, 0.96]) was significantly larger than that of the model using the ACR TI-RADS score alone ($P < 0.001$) (Fig. 3).

In the external validation set, compared with the model using the ACR TI-RADS score (0.84 [95 % CI: 0.79, 0.89]), the AUC of the model using only radiating blood flow signals (0.89 [95 % CI: 0.85, 0.93]; $P = 0.056$) was nominally higher, but the difference was not statistically significant. The AUC of the model using the combination of radiating blood flow signals and the ACR TI-RADS score (0.91 [95 % CI 0.86, 0.95]) was significantly larger than that of the model using the ACR TI-RADS score alone ($P < 0.001$) (Fig. 3). The best cutoff value of the combined model was 9.5 (predicted probability of malignancy: 79.18 %, [95 % CI: 76.06 %, 81.86 %]). The best cutoff value of the ACR TI-RADS model was 6.5 (predicted probability of malignancy: > 20 %). The accuracy, sensitivity, specificity, PPV, and NPV data are shown in Table 4.

Table 3
Association between malignant thyroid nodules and other variables in the training set.

Variables	No. of malignant (%) (n = 1259)	No. of benign (%) (n = 451)	P value	Multi-variate logistic regression analysis	
				OR (95 % CI)	P value
Sex			0.001		
Female	892 (70.8)	356 (78.9)		1.00	
Male	367 (29.2)	95 (21.1)		1.67 (1.03, 2.71)	0.036
Age			<0.001	0.96 (0.95, 0.98)	<0.001
Mean ± SD	42.1 ± 11.3	46.3 ± 12.3			
Median (IQR)	41.0 (34.0, 49.0)	46.0 (37.0, 56.0)			
Composition			<0.001		
Cystic/ Spongiform/ Mixed cystic and solid	12 (1.0)	122 (27.1)		1.00	
Solid	1247 (99.0)	329 (72.9)		4.12 (1.42, 11.95)	0.009
Echogenicity			<0.001		
Anechoic/ Hyper/ *iso*-echoic	44 (3.5)	269 (59.6)		1.00	
Hypoechoic	915 (72.7)	160 (35.5)		3.64 (2.06, 6.45)	<0.001
Very hypoechoic	300 (23.8)	22 (4.9)		3.41 (1.54, 7.54)	0.002
Shape			<0.001		
Wider than tall	816 (64.8)	436 (96.7)		1.00	
Taller than wide	443 (35.2)	15 (3.3)		2.48 (1.28, 4.82)	0.007
Margin			<0.001		
Smooth	32 (2.5)	170 (37.7)		1.00	
Ill-defined	65 (5.2)	136 (30.2)		2.97 (1.44, 6.10)	0.003
Irregular or lobulated	997 (79.2)	139 (30.8)		2.32 (1.23, 4.40)	0.010
Extrathyroidal extension	165 (13.1)	6 (1.3)		8.41 (2.82, 25.13)	<0.001
No echogenic foci or comet-tail artifacts			<0.001		
Absent	543 (43.1)	372 (82.5)		1.00	
Present	716 (56.9)	79 (17.5)		1.21 (0.61, 2.39)	0.584
Macrocalcification			0.765		
Absent	1183 (94.0)	422 (93.6)			
Present	76 (6.0)	29 (6.4)			
Rim calcification			0.113		
Absent	1250 (99.3)	444 (98.4)			
Present	9 (0.7)	7 (1.6)			
Punctate echogenic foci			<0.001		
Absent	620 (49.2)	406 (90.0)		1.00	
Present	639 (50.8)	45 (10.0)		4.69 (2.27, 9.72)	<0.001
Radiating blood flow signals			<0.001		
Absent	142 (11.3)	420 (93.1)		1.00	
Present	1117 (88.7)	31 (6.9)		47.28 (28.22, 79.24)	<0.001

Note: Unless otherwise specified, presented data are the numbers of nodules, with percentages in parentheses. SD = standard deviation; IQR = interquartile range.

4. Discussion

To our knowledge, the morphological characteristics of the blood flow of thyroid nodules, ultrasonic characteristics of radiating blood flow signals, are summaried here in detail for the first time. This study showed that radiating blood flow was an independent risk factor for diagnosing malignant thyroid nodules and had good diagnostic value with an AUC of 0.92 [95 % CI: 0.90, 0.94]. Moreover, radiating blood flow signals significantly improved the diagnostic efficiency of the ACR TI-RADS score from an AUC of 0.92 [95 % CI: 0.90, 0.95] to 0.97 [95 % CI: 0.96, 0.98].

CDUS is the most commonly used method for evaluating the blood flow of thyroid nodules [21]. However, there are still controversial on using vascular abundance and the distribution pattern of blood flow to distinguish benign and malignant thyroid nodules [21]. The morphological characteristics of blood flow in thyroid nodules have been unappreciated to date and are rarely reported [18,19]. In this study, we have made it clear that radiating blood flow is a typical CDUS feature of thyroid cancer, and we found four forms of radiating blood flow (Fig. 1). There are difference in the size of nodules with different form. The mean sizes of nodules with radiating blood flow signals that were presented as form A-D were respectively 0.83 ± 0.53 cm, 0.88 ± 0.48 cm, 1.00 ± 0.54 cm, 1.43 ± 1.12 cm ($P < 0.001$). We found that the larger the nodule, the more radiating blood flow is concentrated in the center of the nodule. Among them, form D was similar to the spoke wheel blood flow signals proposed by Xue et al [19] and found in relatively large thyroid nodules. The mean sizes of nodules with spoke wheel blood flow signals was 2.05 ± 1.09 cm, which is similar to the results in this study. The difference is that the incidence of spoke wheel blood flow signals was only 1 ‰, which was significantly lower than observed in this study (68.1 %). Firstly, we agree with the reason indicated by Xue et al [19], that is the parameters of CDUS were not adjusted during image acquisition. In this study, we paid attention to the adjustment of CDUS parameters and the routine acquisition of multifaceted ultrasound images of thyroid nodules. Therefore, more forms of radiating blood flow signals were found in small nodules, like form A-C. More importantly, people have not paid enough attention to the morphological characteristics of blood flow in thyroid nodules. Jia et al [18] built a Human Artificial Intelligence Hybrid (HAIbrid) integrating framework for nodule malignancy stratification and diagnosis; in doing so, they accidentally identified a second-order feature interaction that has been overlooked by radiologists and in conventional feature selection methods, which was blood flow signals vertically distributed around the nodule that are similar to form B-C in our study. In short, CDUS images

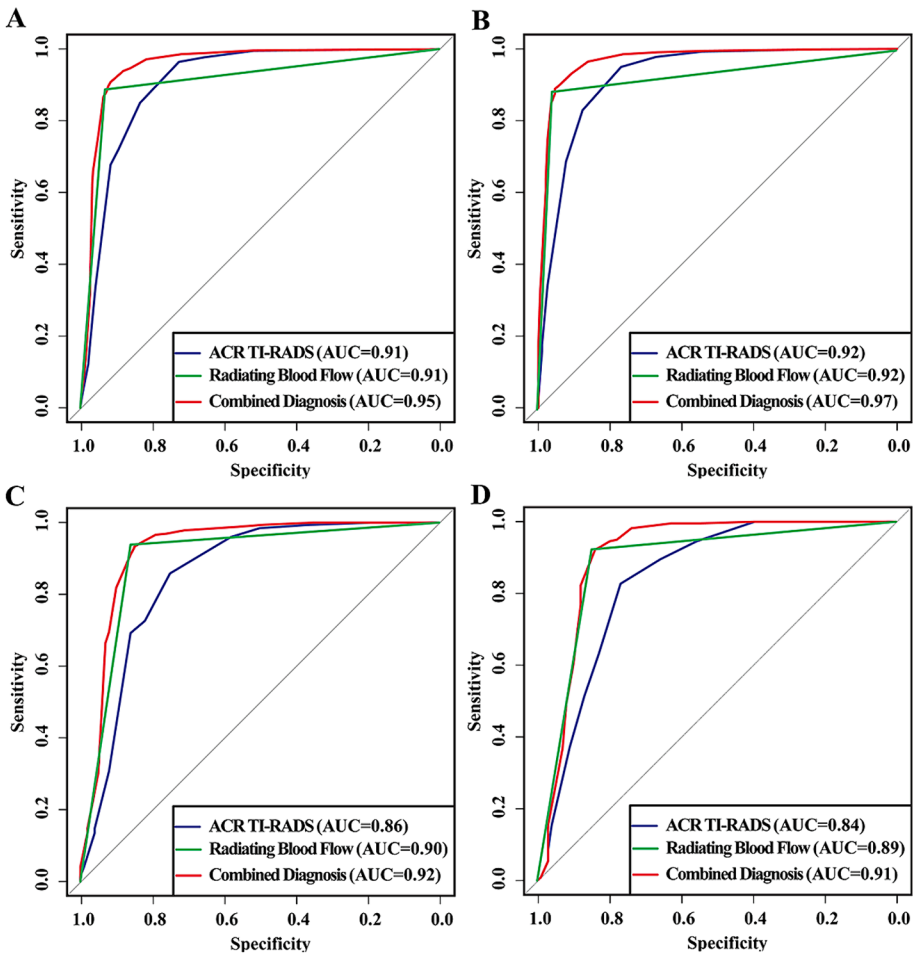

Fig. 3. ROC analysis of the performance of radiologists in the training set (A), internal validation set 1 (B), internal validation set 2 (C) and external validation set (D).

of thyroid nodules contain effective but often neglected information to distinguish benign and malignant thyroid nodules, such as radiating blood flow found in this study. It does not rule out the possibility of other valuable CDUS features being found in the future.

CEUS is considered to be an effective technique for evaluating microvascularization [22]. The European Federation of Societies for Ultrasound in Medicine and Biology (EFSUMB) guideline indicated that the developing foreground of CEUS in thyroid is vast [23]. A meta-analysis on evaluating the diagnostic value of CEUS in differentiating benign and malignant thyroid nodules showed that the pooled sensitivity and specificity of CEUS were 85 % (95 % CI 83 %–88 %) and 82 % (95 % CI 77 %–87 %) respectively [24]. Based on this, a CEUS thyroid imaging reporting and data system built on qualitative nonenhanced US and CEUS features was developed by Ruan et al [15]. It had high diagnostic value with an AUC of 0.93 (95 % CI: 0.92, 0.95), higher than the 0.88 AUC (95 % CI: 0.85, 0.90) of ACR TIRADS. However, CEUS is a high-cost and invasive technology that cannot be widely applied in substrate hospitals without difficulty [25]. CDUS and power Doppler US are traditional vascular imaging technology that is low-cost and non-invasive [26,27]. And microvascular imaging based on Doppler technique (such as superb microvascular imaging and angio planewave ultrasensitive imaging) generates microvascular images resembling those from CEUS without the need of intravenous contrast injection, which can assess the characteristics of blood flow more conveniently [28–31]. Therefore, the morphological characteristics of blood flow on CDUS images will be promoted more extensively.

Xue et al indicated that the spoke-wheel blood flow signal is a highly specific feature of papillary thyroid carcinoma [19]. In this research, 90.1 % (2083/2313) of papillary thyroid carcinoma showed radiating blood flow (Table 2), and the incidences of radiating blood flow in other pathological types of malignant thyroid nodules were all over 50 % (Table 2), with 100 % of squamous cell carcinomas, in particular, showing radiating blood flow. We speculated that radiating blood flow is not the specific ultrasound feature of papillary thyroid carcinoma, but the ultrasound feature of all pathological types of malignant thyroid nodules. However, the sample sizes of other pathological types of thyroid malignant nodules were too small; future studies with larger sample sizes are needed to validate these findings. Currently, the formation mechanism of radiating blood flow is undefined and may be investigated in future research, which is likely to yield interesting findings.

For a new ultrasound feature of thyroid cancer, ease of grasp is extremely important. In this study, six radiologists were trained by a combination of static images and dynamic videos of thyroid nodules. The result showed that training significantly improved six radiologists' accuracy and interobserver consistency of experienced radiologists with regard to feature analysis of radiating blood flow and final assessment. The consistency was increased from 0.03– 0.06 to 0.58–0.91, and accuracy was increased from 34.40 %–40.40 % to 86.40 %–96.40 %. It indicated that the radiating blood flow feature could be mastered after brief training, making it easy to apply in clinical practice in the future. However, compared with the widely accepted grayscale US features, for various forms of radiating blood flow, radiologists may need to spend more energy to master this feature. And during the examination, compared with the adjustment of grayscale US parameters, radiologists may need more patience to adjust CDUS parameters in real time to better visualize the morphology of blood flow in nodules.

Table 4
Comparison of the diagnostic performances of the ACR TI-RADS score, radiating blood flow signals, and their combination in the training set, internal validation set 1, internal validation set 2 and external validation set.

Method	AUC	Accuracy (%)	Sensitivity (%)	Specificity (%)	PPV (%)	NPV (%)	P value*
Training set							
ACR TIRADS	0.91	84.56	84.99	83.37	93.45	66.55	–
	(0.89, 0.93)	(82.76, 86.24)	(82.89, 86.92)	(79.61, 86.69)	(91.86, 94.81)	(62.49, 70.43)	
Radiating blood flow	0.91	89.88	88.72	93.13	97.30	74.73	0.923
	(0.89, 0.92)	(88.36, 91.27)	(86.84, 90.42)	(90.39, 95.28)	(96.19, 98.16)	(70.93, 78.28)	
Combined diagnosis	0.95	90.99	90.79	91.57	96.78	78.07	<0.001
	(0.94, 0.97)	(89.54, 92.31)	(89.05, 92.33)	(88.62, 93.97)	(95.61, 97.71)	(74.30, 81.53)	
Internal validation set 1							
ACR TIRADS	0.92	84.17	82.90	87.69	94.89	65.02	–
	(0.90, 0.95)	(81.33, 86.74)	(79.45, 85.99)	(82.24, 91.95)	(92.50, 96.70)	(58.92, 70.77)	
Radiating blood flow	0.92	90.45	88.48	95.90	98.35	75.10	0.859
	(0.90, 0.94)	(88.09, 92.48)	(85.47, 91.05)	(92.08, 98.21)	(96.77, 99.28)	(69.25, 80.34)	
Combined diagnosis	0.97	91.13	90.15	93.85	97.59	77.54	<0.001
	(0.96, 0.98)	(88.84, 93.09)	(87.31, 92.53)	(89.50, 96.78)	(95.82, 98.75)	(71.68, 82.70)	
Internal validation set 2							
ACR TIRADS	0.86	83.29	85.85	75.00	91.78	61.98	–
	(0.81, 0.91)	(79.40, 86.72)	(81.58, 89.45)	(65.34, 83.12)	(88.10, 94.61)	(52.71, 70.65)	
Radiating blood flow	0.90	92.00	93.85	86.00	95.61	81.13	0.072
	(0.86, 0.94)	(89.00, 94.40)	(90.66, 96.20)	(77.63, 92.13)	(92.75, 97.58)	(72.38, 88.08)	
Combined diagnosis	0.92	91.76	94.46	83.00	94.75	82.18	<0.001
	(0.88, 0.96)	(88.73, 94.20)	(91.39, 96.68)	(74.18, 89.77)	(91.73, 96.91)	(73.30, 89.08)	
External validation set							
ACR TIRADS	0.84	80.88	82.73	76.77	88.78	66.67	–
	(0.79, 0.89)	(76.13, 85.05)	(77.07, 87.48)	(67.21, 84.67)	(83.64, 92.75)	(57.23, 75.22)	
Radiating blood flow	0.89	89.97	92.27	84.85	93.12	83.17	0.056
	(0.85, 0.93)	(86.13, 93.04)	(87.92, 95.43)	(76.24, 91.26)	(88.91, 96.10)	(74.42, 89.88)	
Combined diagnosis	0.91	89.66	92.73	82.83	92.31	83.67	<0.001
	(0.86, 0.95)	(85.78, 92.77)	(88.46, 95.79)	(73.94, 89.67)	(87.97, 95.46)	(74.84, 90.37)	

Note: Data in parentheses are 95 % CIs. ACR TI-RADS = American College of Radiology Thyroid Imaging Reporting and Data System, Combined diagnosis = the combination of radiating blood flow and ACR TI-RADS, AUC = area under the receiver operating characteristic curve, NPV = negative predictive value, PPV = positive predictive value.
* For the comparison of AUCs between the ACR TI-RADS score model and the two other regression models.

It must also be noted that the study had several limitations. First, the inclusion of consecutive patients examined by 5 radiologists who were familiar with radiating blood flow might lead to selection bias. Second, all patients underwent a pathological examination, instead of thyroid nodule screening, at secondary or tertiary hospitals, and the First Affiliated Hospital of Sun Yat-Sen University is a referral center of South China. Some patients who had thyroid nodules with high probability of being benign skipped surgery or FNA though proceeding with follow up. This might explain the higher proportion of malignant thyroid nodules in this study. In addition, the higher proportion of malignant thyroid nodules might explain why the predicted probability of malignancy of the combined model was higher than that of the ACR TI-RADS. Third, among malignant thyroid nodules, other pathological types, except papillary thyroid carcinomas, accounted for a small proportion. Determining whether radiating blood flow is a US feature of these pathological types will require further research with a larger sample size. Fourth, this was a retrospective study, and prospective data are needed to further verify the diagnostic value of radiating blood flow.

In conclusion, radiating blood flow is a new ultrasound feature that is an independent predictor of malignant thyroid nodules that could significantly improve the diagnostic value of ACR TI-RADS.

5. Funding statement

The work was supported by the Key Research and Development Program of Guangzhou Science and Technology Projects (No. 2023B03J1260).

CRediT authorship contribution statement

Sha-Sha Huang: Writing – original draft. **Zheng Yang:** Data curation. **Bin Li:** Methodology. **Zhi-Hao Jiang:** Investigation. **Yang Tan:** Data curation. **Duo-Duo Hao:** Data curation. **Chun-Qiao Chen:** Data curation. **Ying-Wei Wang:** Data curation. **Jin-Yu Liang:** Data curation. **Fu-Shun Pan:** Data curation. **Yi-Hao Liu:** Writing – review & editing. **Xiao-Yan Xie:** Supervision. **Yi-Fan Zhu:** Writing – review & editing. **Zhu Wang:** Writing – review & editing, Conceptualization.

Declaration of competing interest

The authors declare that they have no known competing financial interests or personal relationships that could have appeared to influence the work reported in this paper.

Acknowledgments

We thank Ajiguli Yushan, Yanbing Yao, Ming Zhou, Jinying Fu, Jiali Feng, and Jiaying Hu for helping with interobserver reliability analyses of radiating blood flow signals. We thank Haipeng Xiao, PhD, Sui Peng, PhD, for constructive suggestions and helpful discussion to improve our manuscript.

Appendix A. Supplementary data

Supplementary data to this article can be found online at https://doi.org/10.1016/j.ejrad.2024.111502.

References

[1] J.D. Iannuccilli, J.J. Cronan, J.M. Monchik, Risk for malignancy of thyroid nodules as assessed by sonographic criteria: the need for biopsy, J. Ultrasound Med. 23 (11) (2004) 1455–1464.

[2] H.G. Kim, H.-J. Moon, J.Y. Kwak, E.-K. Kim, Diagnostic accuracy of the ultrasonographic features for subcentimeter thyroid nodules suggested by the revised American Thyroid Association guidelines, Thyroid 23 (12) (2013) 1583–1589.

[3] P.W. Rosario, A.L.d. Silva, M.A.R. Borges, M.R. Calsolari, Is Doppler ultrasound of additional value to gray-scale ultrasound in differentiating malignant and benign thyroid nodules? Arch. Endocrinol. Metab. 59 (1) (2015) 79–83.

[4] F. Fobbe, R. Finke, E. Reichenstein, H. Schleusener, K.J. Wolf, Appearance of thyroid diseases using colour-coded duplex sonography, Eur. J. Radiol. 9 (1) (1989) 29–31.

[5] E. Horvath, S. Majlis, R. Rossi, C. Franco, J.P. Niedmann, A. Castro, M. Dominguez, An ultrasonogram reporting system for thyroid nodules stratifying cancer risk for clinical management, J. Clin. Endocrinol. Metab. 94 (5) (2009) 1748–1751.

[6] D.S. Cooper, G.M. Doherty, B.R. Haugen, R.T. Kloos, S.L. Lee, S.J. Mandel, E. L. Mazzaferri, B. McIver, F. Pacini, M. Schlumberger, S.I. Sherman, D.L. Steward, R. M. Tuttle, Revised American Thyroid Association management guidelines for patients with thyroid nodules and differentiated thyroid cancer, Thyroid 19 (11) (2009) 1167–1214.

[7] J.L. Wémeau, J.L. Sadoul, M. d'Herbomez, H. Monpeyssen, J. Tramalloni, E. Leteurtre, F. Borson-Chazot, P. Caron, B. Carnaille, J. Léger, C. Do, M. Klein, I. Raingeard, R. Desailloud, L. Leenhardt, Guidelines of the French society of endocrinology for the management of thyroid nodules, Ann. Endocrinol. (Paris) 72 (4) (2011) 251–281.

[8] P. Perros, K. Boelaert, S. Colley, C. Evans, R.M. Evans, G. Gerrard Ba, J. Gilbert, B. Harrison, S.J. Johnson, T.E. Giles, L. Moss, V. Lewington, K. Newbold, J. Taylor, R.V. Thakker, J. Watkinson, G.R. Williams, Guidelines for the management of thyroid cancer, Clin. Endocrinol. (Oxf) 81 (Suppl. 1) (2014).

[9] B.R. Haugen, E.K. Alexander, K.C. Bible, G.M. Doherty, S.J. Mandel, Y.E. Nikiforov, F. Pacini, G.W. Randolph, A.M. Sawka, M. Schlumberger, K.G. Schuff, S.I. Sherman, J.A. Sosa, D.L. Steward, R.M. Tuttle, L. Wartofsky, 2015 American Thyroid Association Management Guidelines for Adult Patients with Thyroid Nodules and Differentiated Thyroid Cancer: The American Thyroid Association Guidelines Task Force on Thyroid Nodules and Differentiated Thyroid Cancer, Thyroid 26 (1) (2016).

[10] H. Gharib, E. Papini, J.R. Garber, D.S. Duick, R.M. Harrell, L. Hegedüs, R. Paschke, R. Valcavi, P. Vitti, American association of clinical endocrinologists, American college of endocrinology, and Associazione Medici Endocrinologi medical guidelines for clinical practice for the diagnosis and management of thyroid nodules–2016 update, Endocr. Pract. 22 (5) (2016) 622–639.

[11] J.H. Shin, J.H. Baek, J. Chung, E.J. Ha, J.-H. Kim, Y.H. Lee, H.K. Lim, W.-J. Moon, D.G. Na, J.S. Park, Y.J. Choi, S.Y. Hahn, S.J. Jeon, S.L. Jung, D.W. Kim, E.-K. Kim, J.Y. Kwak, C.Y. Lee, H.J. Lee, J.H. Lee, J.H. Lee, K.H. Lee, S.-W. Park, J.Y. Sung, Ultrasonography diagnosis and imaging-based management of thyroid nodules: revised korean society of thyroid radiology consensus statement and recommendations, Korean J. Radiol. 17 (3) (2016) 370–395.

[12] F.N. Tessler, W.D. Middleton, E.G. Grant, J.K. Hoang, L.L. Berland, S.A. Teefey, J. J. Cronan, M.D. Beland, T.S. Desser, M.C. Frates, L.W. Hammers, U.M. Hamper, J. E. Langer, C.C. Reading, L.M. Scoutt, A.T. Stavros, ACR thyroid imaging, reporting and data system (TI-RADS): white paper of the ACR TI-RADS committee, J. Am. Coll. Radiol. 14 (5) (2017) 587–595.

[13] G. Russ, S.J. Bonnema, M.F. Erdogan, C. Durante, R. Ngu, L. Leenhardt, European thyroid association guidelines for ultrasound malignancy risk stratification of thyroid nodules in adults: the EU-TIRADS, Eur. Thyroid J. 6 (5) (2017) 225–237.

[14] J. Zhou, L. Yin, X. Wei, S. Zhang, Y. Song, B. Luo, J. Li, L. Qian, L. Cui, W. Chen, C. Wen, Y. Peng, Q. Chen, M. Lu, M. Chen, R. Wu, W. Zhou, E. Xue, Y. Li, L. Yang, C. Mi, R. Zhang, G. Wu, G. Du, D. Huang, W. Zhan, 2020 Chinese guidelines for ultrasound malignancy risk stratification of thyroid nodules: the C-TIRADS, Endocrine 70 (2) (2020) 256–279.

[15] J. Ruan, X. Xu, Y. Cai, H. Zeng, M. Luo, W. Zhang, R. Liu, P. Lin, Y. Xu, Q. Ye, B. Ou, B. Luo, A practical CEUS thyroid reporting system for thyroid nodules, Radiology 305 (1) (2022) 149–159.

[16] W.-J. Moon, J.H. Baek, S.L. Jung, D.W. Kim, E.K. Kim, J.Y. Kim, J.Y. Kwak, J. H. Lee, J.H. Lee, Y.H. Lee, D.G. Na, J.S. Park, S.W. Park, Ultrasonography and the ultrasound-based management of thyroid nodules: consensus statement and recommendations, Korean J. Radiol. 12 (1) (2011).

[17] H. Khadra, M. Bakeer, A. Hauch, T. Hu, E. Kandil, Is vascular flow a predictor of malignant thyroid nodules? A meta-Analysis, Gland Surg. 5 (6) (2016) 576–582.

[18] X. Jia, Z. Ma, D. Kong, Y. Li, H. Hu, L. Guan, J. Yan, R. Zhang, Y. Gu, X. Chen, L. Shi, X. Luo, Q. Li, B. Bai, X. Ye, H. Zhai, H. Zhang, Y. Dong, L. Xu, J. Zhou, Caau, Novel human artificial intelligence hybrid framework pinpoints thyroid nodule malignancy and identifies overlooked second-order ultrasonographic features, Cancers (Basel) 14 (18) (2022).

[19] N. Xue, P. Li, H. Deng, J. Yi, Y. Xie, S. Zhang, The spoke wheel color Doppler blood flow signal is a specific sign of papillary thyroid carcinoma, Front. Endocrinol. (Lausanne) 13 (2022) 1030143.

[20] R.B. D'Agostino, S. Grundy, L.M. Sullivan, P. Wilson, Validation of the Framingham coronary heart disease prediction scores: results of a multiple ethnic groups investigation, J. Am. Med. Assoc. 286 (2) (2001) 180–187.

[21] J. Chung, Y.J. Lee, Y.J. Choi, E.J. Ha, C.H. Suh, M. Choi, J.H. Baek, D.G. Na, Clinical applications of Doppler ultrasonography for thyroid disease: consensus statement by the Korean Society of Thyroid Radiology, Ultrasonography 39 (4) (2020) 315–330.

[22] J. Zhan, H. Ding, Application of contrast-enhanced ultrasound for evaluation of thyroid nodules, Ultrasonography 37 (4) (2018) 288–297.

[23] P.S. Sidhu, V. Cantisani, C.F. Dietrich, O.H. Gilja, A. Saftoiu, E. Bartels, M. Bertolotto, F. Calliada, D.-A. Clevert, D. Cosgrove, A. Deganello, M. D'Onofrio, F.M. Drudi, S. Freeman, C. Harvey, C. Jenssen, E.-M. Jung, A.S. Klauser, N. Lassau, M.F. Meloni, E. Leen, C. Nicolau, C. Nolsoe, F. Piscaglia, F. Prada, H. Prosch, M. Radzina, L. Savelli, H.-P. Weskott, H. Wijkstra, The EFSUMB guidelines and recommendations for the clinical practice of contrast-enhanced ultrasound (CEUS) in non-hepatic applications: update 2017 (Long Version), Ultraschall. Med. 39 (2) (2018).

[24] P. Trimboli, M. Castellana, C. Virili, R.F. Havre, F. Bini, F. Marinozzi, F. D'Ambrosio, F. Giorgino, L. Giovanella, H. Prosch, G. Grani, M. Radzina, V. Cantisani, Performance of contrast-enhanced ultrasound (CEUS) in assessing thyroid nodules: a systematic review and meta-analysis using histological standard of reference, Radiol. Med. 125 (4) (2020) 406–415.

[25] V. Cantisani, M. Bertolotto, H.P. Weskott, L. Romanini, H. Grazhdani, M. Passamonti, F.M. Drudi, F. Malpassini, A. Isidori, F.M. Meloni, F. Calliada, F. D'Ambrosio, Growing indications for CEUS: the kidney, testis, lymph nodes, thyroid, prostate, and small bowel, Eur J Radiol 84 (9) (2015) 1675–1684.

[26] J. Bojunga, P. Trimboli, Thyroid ultrasound and its ancillary techniques, Rev. Endocr. Metab. Disord. 25 (1) (2024) 161–173.

[27] D.N. White, Johann Christian Doppler and his effect–a brief history, Ultrasound Med. Biol. 8 (6) (1982) 583–591.

[28] L. Jiang, D. Zhang, Y.-N. Chen, X.-J. Yu, M.-F. Pan, L. Lian, The value of conventional ultrasound combined with superb microvascular imaging and color Doppler flow imaging in the diagnosis of thyroid malignant nodules: a systematic review and meta-analysis, Front. Endocrinol. (Lausanne) 14 (2023) 1182259.

[29] H. Luo, L. Yin, Diagnostic value of superb microvascular imaging and color doppler for thyroid nodules: a meta-analysis, Front. Oncol. 13 (2023) 1029936.

[30] H.S. Ahn, J.B. Lee, M. Seo, S.H. Park, B.I. Choi, Distinguishing benign from malignant thyroid nodules using thyroid ultrasonography: utility of adding superb microvascular imaging and elastography, Radiol. Med. 123 (4) (2018) 260–270.

[31] G. Guo, J. Feng, C. Jin, X. Gong, Y. Chen, S. Chen, Z. Wei, H. Xiong, J. Lu, a novel nomogram based on imaging biomarkers of shear wave Elastography, Angio Planewave ultrasensitive imaging, and conventional ultrasound for preoperative prediction of malignancy in patients with breast lesions, Diagnostics (Basel) 13 (3) (2023).